Advances in Nano Research, *Vol. 19, No. 4 (2025) 399-410*
https://doi.org/10.12989/anr.2025.19.4.399

Influence of nonlinear distribution CNT and variable viscoelastic foundation on wave propagation in composite beams

Djaloul Zarga*[1], Mokhtar Nebab[1,2], Hassen Ait Atmane[2,3] and Hadji Lazreg[4,5]

[1]*Department of Civil Engineering, Faculty of Technology, University of M'Hamed BOUGARA Boumerdes, Algeria.*
[2]*Laboratory of Structures, Geotechnics and Risks, Department of Civil Engineering, Hassiba Benbouali University of Chlef, Algeria*
[3]*Department of Civil Engineering, Faculty of Civil Engineering and Architecture, University Hassiba Benbouali of Chlef, Algeria*
[4]*Faculty of Civil Engineering, Ton Duc Thang University, Ho Chi Minh City, Vietnam*
[5]*Laboratory of Geomatics and Sustainable Development, Ibn Khaldoun University of Tiaret, Tiaret, Algeria*

(*Received June 5, 2025, Revised September 25, 2025, Accepted September 29, 2025*)

Abstract. In this study, the propagation of waves in beams reinforced with carbon nanotube-reinforced composites (CNTRCs) resting on a variable viscoelastic foundation is examined. The novelty of this work lies in addressing CNTRC beams resting on a spatially variable viscoelastic foundation, a problem that has received limited attention in the literature despite its practical significance. The reinforcement is provided by single-walled carbon nanotubes (SWCNTs), distributed in various configurations of uniaxially aligned material. Particular attention is given to the uniform distribution (UD) of reinforcement, which is analyzed to evaluate the effects of non-linear (NL) variation in CNT distribution. The governing equations of motion for the CNTRC beam are derived through the application of the First-Order Shear Deformation Theory (FSDT) in conjunction with Hamilton's principle. The beam is considered to be functionally graded (FG) and is modeled as resting on a three-parameter viscoelastic foundation, incorporating a Winkler spring interconnected with a Pasternak shear layer. Moreover, the viscoelastic behavior of the foundation is included, and the spatial variability of the Winkler foundation stiffness along the beam length is represented using linear, sinusoidal, and parabolic distributions. Analytical solutions in the form of dispersion relations are obtained to determine the wave frequencies and phase velocities. The influence of different CNT distribution configurations on wave propagation characteristics is demonstrated. Furthermore, the effects of CNT volume fraction, foundation stiffness parameters, and the damping coefficient on the dynamic response of the system are systematically investigated. Overall, this study advances the understanding of wave propagation in CNTRC beams by explicitly incorporating both non-linear CNT distribution and spatially variable viscoelastic foundations, offering insights not captured in previous beam models.
Keywords: carbon nanotube; FG-CNT beams; viscoelastic foundation; wave propagation

1. Introduction

The reinforcement of beams with carbon nanotubes has wide-ranging applications across various industries, including aerospace, automotive, civil engineering, and structural design. In aerospace applications (Djilali Djebbour *et al*. 2024, Syduzzaman *et al*. 2025), CNT-reinforced beams can contribute to the development of lightweight and high-strength structures for aircraft and spacecraft. In civil engineering, they can be utilized in the construction of bridges, buildings, and other infrastructure to enhance structural integrity and durability.

Carbon nanotubes (CNTs) are exceptional candidates for reinforcing polymer composites due to their high elastic modulus, tensile strength, low density, and high aspect ratio (Thostenson *et al*. 2001, Lau and Hui 2002). Their potential applications span reinforcing composites, high-performance structural materials, and multifunctional composites, particularly in aerospace (Yamamoto *et al*. 2012). A critical challenge lies in enhancing the dispersion and alignment of CNTs within polymer matrices, which has been addressed through techniques like ex situ methods, force and magnetic fields, electro-spinning, and liquid crystalline phase induction (Xie *et al*. 2005). The mechanical properties of CNT-reinforced composites (CNTRCs) have been extensively studied experimentally, analytically, and numerically. In particular, Hu *et al*. (2005) evaluated macroscopic elastic properties by analyzing representative volume elements under various loads, while Han and Elliott (2007) used molecular dynamics to simulate polymer/CNT composite elasticity. Nejati *et al*. (2016) studied CNT-reinforced beams' buckling and vibration, while Mehar and Panda (2016) analyzed the thermoelastic response of CNT-reinforced plates. More recently, (Asgari *et al*. 2022) explored the dynamic instability of sandwich beams with GPL-reinforced face sheets. Further studies include advanced finite element models for CNT-reinforced microplate buckling (Nguyen *et al*. 2025) and dynamic analysis of hybrid plates (Tao *et al*. 2025). These investigations underscore the ongoing efforts to characterize these innovative materials.

Several studies have focused on the mechanical behavior of composite structures. Wattanasakulpong and Ungbhakorn (2013) examined the static and dynamic behaviors of CNT-RC beams resting on an elastic

*Corresponding author, Ph.D.,
E-mail: nebmokhtar@gmail.com

ISSN: 2287-237X (Print), 2287-2388 (Online)

foundation, while (Lin and Xiang 2014) utilized analytical models such as the First-Order Shear Deformation Beam Theory (FSDBT) and Third-Order Shear Deformation Beam Theory (TSDBT) along with Ritz's method to analyze their vibrational characteristics. Ke *et al.* (2010) investigated the nonlinear free vibrations of FG-CNTRC Timoshenko beams with both symmetric and asymmetric CNT distributions using the Ritz method. (Setoodeh *et al.* 2019) investigate the vibrational behavior of doubly curved sandwich shells with FG-CNTRC face sheets and an FG porous core. Their study reveals how the core porosity, face sheet material gradation, and boundary conditions influence the vibrational characteristics of the structure.

Dynamic and wave propagation studies have also been explored in various CNT-reinforced structures. Ghayoumizadeh *et al.* (2013) investigated transient dynamic analysis and elastic wave propagation in FG-CNTRC structures using the Meshless Local Petrov–Galerkin (MLPG) method. Yas and Samadi (2012) explored both buckling and free vibration of CNTRC Timoshenko beams resting on an elastic foundation, while Wu *et al.* (2015) analyzed vibration and buckling in sandwich beams composed of FG-CNTRC layers. This study investigates the free vibration behavior of functionally graded (FG) beams with bi-directional power-law material distribution using Refined Shear Deformation Theory (Zouatnia *et al.* 2024). Similarly, Kenza Djilali *et al.* (2025) focus on the stability and vibration analysis of shear deformable FG-CNTRC beams supported by elastic foundations. Ghorbanpour Arani *et al.* (2016) analyzed wave propagation in functionally graded carbon nanotube-reinforced piezoelectric microplates using a viscoelastic quasi-3D sinusoidal shear deformation theory.

Despite these extensive studies on Advanced composite beams and plates, there remains a gap in the literature concerning the wave propagation and dynamic response of FG-CNT beams resting on a viscoelastic foundation. The viscoelastic foundation introduces additional damping and stiffness effects, which significantly influence the beam's vibrational and wave propagation characteristics. Previous studies, such as those by Pouresmaeeli *et al.* (2013), have considered viscoelastic effects in nanoplate vibration analysis, but a comprehensive study on FG-CNT beams in this context is still lacking. Frahlia *et al.* (2023) employed a novel higher-order shear deformation theory (HSDT) to assess the influence of viscoelastic foundation parameters on the dynamic response of FG plates. Kolahchi *et al.* (2017) examined wave propagation in FG-CNT-reinforced viscoelastic sandwich plates with integrated sensor-actuator layers using refined zigzag theory. Their study highlights the impact of CNT distribution, foundation parameters, and control layers on dynamic response and wave control efficiency.

Despite extensive studies on the behavior response of CNT-reinforced beams, limited attention has been given to their vibration and wave propagation behavior, especially in functionally graded CNT composites supported by viscoelastic foundations with spatial variability. Previous works have often relied on simplified shear theories or neglected the combined influence of CNT distribution patterns and foundation heterogeneity, leaving a gap in accurately capturing both vibrational and dispersive wave characteristics of such advanced structures. To address this gap, the present study investigates the vibration and wave propagation response of FG-CNT beams supported by viscoelastic foundations using the integral First-Order Shear Deformation Theory (FSDT). The use of the integral-first shear deformation theory (I-FSDT) in this work is intended as an alternative formulation to the classical FSDT. Its purpose is to test and verify the results, offering a complementary solution technique rather than a replacement of ordinary models. By applying Hamilton's principle, equations of motion are derived, and dispersion relations are developed to obtain natural frequencies, wave frequencies, and phase velocities. The accuracy of the proposed formulation is verified through comparison with benchmark results, and the effects of CNT distribution, volume fraction, gradient index, and foundation variability on both vibration and wave propagation responses are systematically examined.

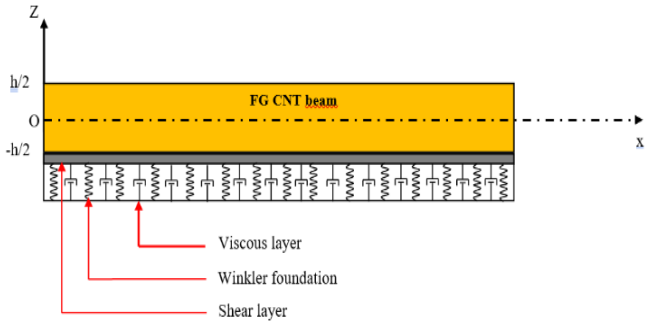

Fig. 1 Geometry of a CNT-RC beam on viscoelastic foundation

2. Effective material properties of CNTRCs

2.1 Effective properties of CNTRC

In this study, the beam is modeled as a composite structure consisting of two constituent materials: an isotropic polymer matrix and single-walled carbon nanotubes (SWCNTs). The beam is assumed to be simply supported and resting on a Winkler–Pasternak elastic foundation (Fig. 1). Five configurations of CNT-reinforced composite beams are investigated, namely the UD, FG-O, FG-X, FG-V, and FG-Λ types, as illustrated in Fig. 2.

For functionally graded CNT-reinforced composite (FG-CNT) beams, the effective material properties, such as Young's modulus and shear modulus, are evaluated using the rule of mixtures, incorporating efficiency parameters to account for nanoscale effects of CNT reinforcement.

$$E_{11} = \eta_1 E_{11}^{cnt} V_{cnt} + V_p E_p \tag{1a}$$

$$\frac{\eta_2}{E_{22}} = \frac{V_{cnt}}{E_{22}^{cnt}} + \frac{V_P}{E_P} \tag{1b}$$

$$\frac{\eta_3}{G_{12}} = \frac{V_{cnt}}{G_{12}^{cnt}} + \frac{V_P}{G_P} \tag{1c}$$

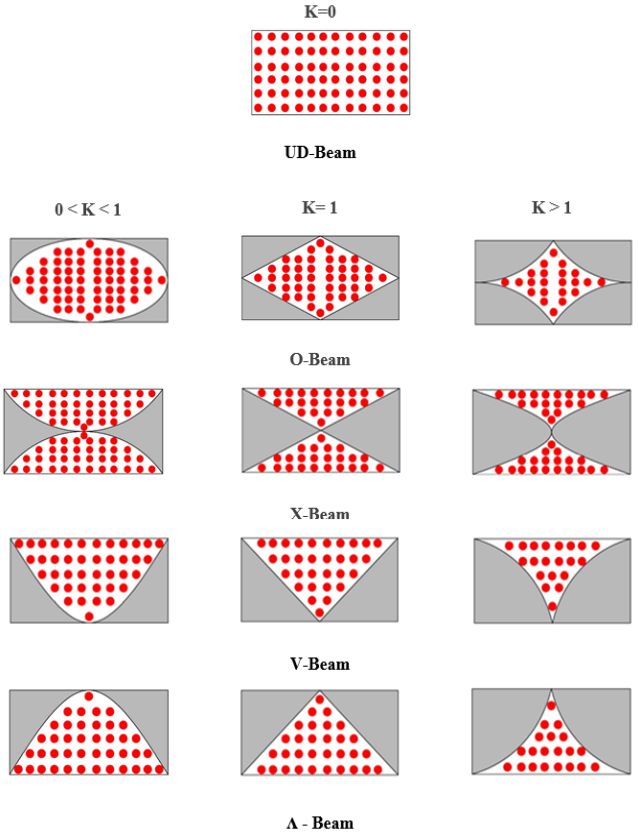

Fig. 2 The various models of the CNT distribution through the thickness of the beam

Table 1 efficiency parameters η_i associated to the volume fractions V_{cnt}^*

V_{cnt}^*	0.12	0.17	0.28
η_1	1.2833	1.3414	1.3228
η_2	1.0566	1.7101	1.7380
η_3	1.0566	1.7101	1.7380

Here, E_{11}^{cnt} , E_{22}^{cnt} , and G_{12}^{cnt} are the longitudinal and transverse Young's moduli and the shear modulus of the CNTs, respectively. The terms V_{CNT} and V_P represent the volume fractions of CNTs and the polymer matrix, which satisfy the relation: V_{CNT}+V_P=1. Similarly, EP and G_P denote the Young's and shear moduli of the polymer matrix. The parameters $\eta_i(i = 1,2,3)$ represent the efficiency factors of the carbon nanotube (CNT). These parameters account for the scale-dependent properties of single-walled carbon nanotubes (SWCNTs). Using a combination of the mixture law and molecular dynamics (MD) simulations, the efficiency parameters of the CNT were calculated (Han and Elliott 2007). The specific values of $\eta_i(i = 1,2,3)$ are abstracted in the Table 1 and showing I the Fig. 2.

The volume fraction of the formulations of the CNT through the thickness can be given as

UD $$V_{cnt} = V_{cnt}^* \tag{2a}$$

FG-O-beam $$V_{cnt} = (K+1)(1-\frac{2|z|}{h})^K V_{cnt}^* \tag{2b}$$

FG-X-beam $$V_{cnt} = (K+1)(\frac{2|z|}{h})^K V_{cnt}^* \tag{2c}$$

FG-V-beam $$V_{cnt} = (K+1)(\frac{1}{2}+\frac{z}{h})^K V_{cnt}^* \tag{2d}$$

FG-Λ-beam $$V_{cnt} = (K+1)(\frac{1}{2}-\frac{z}{h})^K V_{cnt}^* \tag{2e}$$

here, V^*_{CNT} denotes the reference CNT volume fraction, h is the beam thickness, z is the thickness coordinate measured from the mid-plane, and K is the distribution index parameter that governs the degree of CNT gradation through the thickness. The parameter K controls the shape of the CNT distribution: for $0<K<1$ or $K>1$, the distribution is nonlinear, while for $K=0$ it becomes uniform across the section, and for $K=1$ it corresponds to a linear distribution.

The mass density and Poisson's ratio of beams are evaluated following the same homogenization procedure used for the effective elastic moduli. The overall density is obtained from the rule of mixtures, accounting for the contributions of both CNTs and the polymer matrix. Similarly, the effective Poisson's ratio is calculated by weighting the properties of the constituents according to their respective volume fractions.

$$\rho = V_{cnt}\rho^{cnt} + V_P\rho^p \tag{3a}$$

$$\nu = V_{cnt}\nu^{cnt} + V_P\nu^p \tag{3b}$$

where ρ^{cnt}, ρ^p and V^{cnt}, ρ^p are the masse density and poison's ratio of the CNT and the polymer matrix, respectively.

The fraction volume V_{cnt}^* of the CNT is obtained from the following expression

$$V_{cnt}^* = \frac{w_{cnt}}{w_{cnt} + (\frac{\rho_{cnt}}{\rho})(1-w_{cnt})} \tag{4}$$

2.2 Kinematics

In this work, based on Timoshenko's beam hypothesis, the kinematics of the model are expressed as follows:

$$u(x,z,t) = u_0(x,y) + z\varphi_x(x,t) \tag{5a}$$

$$w(x,z,t) = w_0(x,t) \tag{5b}$$

where (u_0, w_0 and φ_x) are three unknown displacements of the mid-plane of the CNT-RC beam.By replacing the rotations of the (x,z) caused by shear, $\varphi_x = \int \theta(x,t)dx$, the displacement field of the present model can be expressed in the undetermined integral form as

$$u(x,z,t) = u_0(x,y) - zk_1\int \theta(x,t)dt \tag{6a}$$

$$w(x,z,t) = w_0(x,t) \tag{6b}$$

where the coefficient "k_1" depend on the geometry.

The non-zero linear strains relations associated with t he displacements $u(x,z,t)$ and $w(x,z,t)$ are as follows

$$\varepsilon_x = \frac{\partial u_0}{\partial x} - zk_1A'\frac{\partial^2\theta}{\partial x^2} \tag{7a}$$

$$\gamma_{xz} = \frac{\partial w_0}{\partial x} - k_1 A' \frac{\partial \theta}{\partial x} \tag{7b}$$

The undetermined integral $\int \theta \, dx$ introduced in the previous section is resolved according to the employed solution type. In the present case, it can be expressed in derivative form as:

$$\int \theta \, dx = A' \frac{\partial \theta}{\partial x} \tag{8a}$$

For a special solution corresponding to harmonic wave propagation of the beam resting on a variable elastic foundation, the assumed displacement form given in Eq. (22) is employed. In this case, we have:

$$\int \theta \, dx = \frac{1}{i\kappa}\theta, \qquad \frac{\partial^2 \theta}{\partial x} = i\kappa\theta \tag{8b}$$

By eliminating θ, the relation becomes

$$\int \theta \, dx = -\frac{1}{\kappa^2}\frac{\partial^2 \theta}{\partial x} \tag{9a}$$

Therefore, the coefficient *A*' are obtained according to the present type of solution utilized. Therefore, the coefficients *A*' and k_1 are expressed as follows:

$$A' = -\tfrac{1}{\kappa^2}, \; k_1 = \kappa^2 \tag{9b}$$

Here, κ denotes the wave number corresponding to propagation along the x-axis. It is important to emphasize that k_1 is not just a numerical factor but a governing displacement-field coefficient (see Eq. (6)) that directly calibrates the contribution of shear deformation in wave and vibration propagation analyses. Unlike the constant shear correction factor typically employed in classical FSDT, the present formulation derives k_1 directly from the harmonic solution, making it explicitly dependent on the wave number *κ*. This dependence allows the model to naturally capture wave–number–sensitive shear effects, thereby linking the kinematic assumptions of Eq. (6) with the integral-first formulation of Eq. (9). As a result, the present approach enhances physical reliability while maintaining full consistency with the assumed displacement field.

The stress-strain relations can be expressed based on the Hooke's relation as

$$\sigma_x = Q_{11}(\varepsilon_x), \; \tau_x = k_s Q_{55}\gamma_s \tag{10a}$$

$$Q_{11}(z) = \tfrac{E_{11}(z)}{1-\nu^2}, \; Q_{55}(z) = G_{12}(z) \tag{10b}$$

where $k_s$represent the shear correction factor and it takes a value ($k_s = 5/6$).

2.3 Equations of motion

The three equations of motion are determined using the Hamilton's principle. The principle can be expressed in the analytical form as (Kehli *et al*. 2024, Mellal *et al*. 2024, Nebab *et al*. 2024)

$$\int_{t_1}^{t_2} (\delta U - \delta K + \delta U_{ef}) \, dt = 0 \tag{11}$$

where δU, δK and δU_{ef} are the variations of the virtual strain energy, virtual kinetic energy and the variation of the potential energy of the viscoelastic foundation, respectively.

The variation of strain energy δU associated to the present model (Eq. (6)) is given as

$$\begin{aligned} \delta U &= \int_0^L \int_A (\sigma_x \, \delta\varepsilon_x + \tau_{xz}\delta\gamma_{xz}) dA dx \\ &= \int_0^L (N_x \frac{\delta\partial u_0}{\partial x} - (k_1 A')M_x \, \delta\frac{\partial^2 \theta}{\partial x^2} \\ &\quad -(k_1 A')Q_x \frac{\delta\partial\theta}{\partial x} + Q_x \frac{\delta\partial w_0}{\partial x}) dA \end{aligned} \tag{12}$$

$$(N_x, M_x) = \textstyle\int_{-h/2}^{h/2} (1, z)\sigma_x \, dz, \; Q_x = \int_{-h/2}^{h/2} \tau_{xz} \, dz \tag{13}$$

The kinetic energy variation δK can be expressed as

$$\begin{aligned} \delta K &= \iint \rho(\dot{u}\,\delta\dot{u} + \dot{w}\delta\dot{w}) dx dz \\ &= \iint \rho \begin{bmatrix} (\dot{u}_0 - z k_1 A' \frac{\partial\dot{\theta}}{\partial x})\delta(\dot{u}_0 - z k_1 A' \frac{\partial\dot{\theta}}{\partial x}) \\ +\dot{w}_0 \delta\dot{w}_0 \end{bmatrix} dx dz \\ &= \int_0^L \begin{Bmatrix} I_0(\dot{u}_0\delta\dot{u}_0 + \dot{w}_0\delta\dot{w}_0) - \\ k_1 A' I_1(\dot{u}_0 \frac{\delta\partial\dot{\theta}}{\partial x} + \frac{\partial\dot{\theta}}{\partial x}\delta\dot{u}_0) \\ +(k_1 A')^2 I_2 \frac{\partial\dot{\theta}}{\partial x}\frac{\delta\partial\dot{\theta}}{\partial x} \end{Bmatrix} dx \end{aligned} \tag{14}$$

With

$$(I_0, I_1, I_2) = \int_{-h/2}^{h/2} \rho(1, z, z^2) dz \tag{15}$$

The external virtual works δV can be expressed as

$$\delta U_{ef} = \iint f_e \, \delta w dx dz \tag{16}$$

where f_e are the reaction force of the foundation. The foundation reaction can be given as

$$f_e = K_w w - K_s \frac{\partial^2 w}{\partial x^2} + C_d \frac{\partial w}{\partial t} \tag{17}$$

where K_w and K_s are the constants of elastic foundations Winkler and Pasternak, respectively. With

$$K_w = \tfrac{\beta_w(x) A_{110}}{L^2}, \; K_s = \beta_s A_{110} \tag{18a}$$

$$\beta_w(x) = \frac{\beta_w}{L^2}\begin{cases} 1 + \Psi(\bar{x}) & \text{Linear} \\ 1 + \Psi(\bar{x})^2 & \text{Parabolic} \\ 1 + \Psi(sin(\pi\bar{x})) & \text{Sinusoidal} \end{cases} \tag{18b}$$

where, β_w and Ψ are the constant and variable elastic foundation parameters, respectively (Nebab *et al*. 2019a, b, 2024, Mokhtar *et al*. 2024a, b). The parameter β_w characterizes the baseline stiffness of the elastic foundation, while Ψ governs the degree of its spatial variation along the beam axis. Note that if Ψ = 0, the elastic foundation reduces to the classical uniform foundation model. This formulation therefore enables the investigation of both uniform and non-uniform foundation conditions within a unified framework.

A_{110} is the extension stiffness of the A_{11} of the

Table 2 The properties of the Poly methacrylate "PMMA" and armchair (10, 10) SWCNTs properties

Polymethacrylate "PMMA"	$E_p = 2.5GPa\ \ \rho_p = 1190\ kg/m^3,$ $\nu^p = 0.3$
Armchair (10, 10) SWCNTs	$E_{11}^{CNT} = 600GPa,\ \rho_{CNT} = 1400\ \ kg/m^3,\ E_{22}^{CNT} = 10GPa,\ \nu^{CNT} = 0.19,$ $G_{12}^{CNT} = 17.2GPa$

polymer only and can be defined as (Yas and Samadi 2012, Kenza Djilali *et al*. 2025) :

$$A_{110} = \int_{-h/2}^{h/2} \frac{E_p}{1-\nu_p} dz \tag{19}$$

Using the Eqs. (12-14), (16) and (17), integrating by part and separating the terms of displacements. The three equations of motion are obtained as

$$\delta u_0: \quad \frac{\partial N_x}{\partial x} = I_0 \ddot{u_0} - (k_1 A')I_1 \frac{\partial \ddot{\theta}}{\partial x}, \tag{20a}$$

$$\delta w_0: \quad \frac{\partial Q_x}{\partial x} - K_w w_0 + K_s \frac{\partial^2 w_0}{\partial x^2} = I_0 \times \ddot{w_0} + C_d \dot{w_0}, \tag{20b}$$

$$\delta \theta: \quad (k_1 A')\frac{\partial^2 M_x}{\partial x^2} - (k_1 A')\frac{\partial Q_x}{\partial x} = (k_1 A') \times I_1 \frac{\partial \ddot{u_0}}{\partial x} - (k_1 A')^2 I_2 \frac{\partial^2 \ddot{\theta}}{\partial x^2}, \tag{20c}$$

Substituting Eqs. (7) and (10) into Eqs. (20) yields,

$$\delta u_0: \quad A_{11}\frac{\partial^2 u_0}{\partial x^2} - (k_1 A')B_{11}\frac{\partial^3 \theta}{\partial x^3} = I_0 \ddot{u_0} - (k_1 A')I_1 \frac{\partial \ddot{\theta}}{\partial x}, \tag{20d}$$

$$\delta w_0: \quad (A_{55}^s + K_s)\frac{\partial^2 w_0}{\partial x^2} - (k_1 A')A_{55}^s \frac{\partial^2 \theta}{\partial x^2} - K_w w_0 = I_0 \ddot{w}_0 + C_d \dot{w}_0, \tag{20e}$$

$$\delta \theta: \quad (k_1 A')B_{11}\frac{\partial^3 u_0}{\partial x^3} - (k_1 A')A_{55}^s \frac{\partial^2 w_0}{\partial x^2} - (k_1 A')^2 D_{11}\frac{\partial^4 \theta}{\partial x^4} + A_{55}^s (k_1 A')^2 \times \frac{\partial^2 \theta}{\partial x^2} = (k_1 A')I_1 \frac{\partial \ddot{u_0}}{\partial x} - (k_1 A')^2 I_2 \frac{\partial^2 \ddot{\theta}}{\partial x^2}, \tag{20f}$$

where A_{11}, B_{11} and D_{11} are the beam stiffness, defined by

$$(A_{11}, B_{11}, D_{11}) = \int_{-h/2}^{h/2} Q_{11}\,(1, z, z^2)dz, \quad A_{55}^s = \int_{-h/2}^{h/2} k_s Q_{55}\, dz \tag{21}$$

3. Dispersion relations

The solution representing wave propagation in an infinite functionally graded plate is assumed to take the following form:

$$\begin{Bmatrix} u_0 \\ w_0 \\ \theta \end{Bmatrix} = \begin{Bmatrix} U \\ W \\ X \end{Bmatrix} e^{i(\kappa\ \ x - \omega t)} \tag{22}$$

U, W and X are the amplitudes of the waves, ω is the circular frequency, and I is the imaginary number. Using this solution, the three governing equations are rewritten in the following matrix form

$$\left(\begin{bmatrix} k_{11} & k_{12} & k_{13} \\ k_{12} & k_{22} & k_{23} \\ k_{31} & k_{32} & k_{33} \end{bmatrix} - \omega^2 \times \begin{bmatrix} m_{11} & m_{12} & m_{13} \\ m_{12} & m_{22} & m_{23} \\ m_{31} & m_{32} & m_{33} \end{bmatrix} - \omega \begin{bmatrix} 0 & 0 & 0 \\ 0 & iC_d & 0 \\ 0 & 0 & 0 \end{bmatrix} \right) \begin{Bmatrix} U \\ W \\ X \end{Bmatrix} = 0 \tag{23}$$

where

$$k_{11} = A_{11}(i\kappa)^2,\ \ k_{12} = k_{21} = 0, \quad k_{13} = k_{31} = B_{11}(k_1 A')(i\kappa)^3 \tag{24a}$$

$$k_{22} = (A_{55}^S + K_s)(i\kappa)^2 - K_w, \quad k_{23} = k_{32} = -A_{55}^s (k_1 A')(i\kappa)^2 \tag{24b}$$

$$k_{33} = A_{55}^s (k_1 A')^2 (i\kappa)^2 - D_{11}(k_1 A')(i\kappa)^4 \tag{24c}$$

$$m_{11} = I_0 (i)^2, m_{12} = m_{21} = 0, \quad m_{13} = m_{31} = -(k_1 A')(i\kappa)(i)^2 I_1 \tag{25a}$$

$$m_{22} = I_0 (i)^2,\ \ m_{23} = m_{32} = 0 \tag{25b}$$

$$m_{33} = -I_2 (k_1 A')^2 (i\kappa)^2 (i)^2 \tag{25c}$$

Three frequencies are found as functions of the wavenumbers

$$\omega_i = W_i(\kappa), (i = 1,2,3) \tag{26}$$

For dynamic analysis

$$\varpi = WL\sqrt{\frac{I_{00}}{A_{110}}} \tag{27}$$

where I_{00} is the extension inertia of the I_0 of the polymer only.

The phase velocity is simply the frequency divided by the corresponding wavenumber.

$$C_i = \frac{W_i(\kappa)}{\kappa} \tag{28}$$

4. Results and discussion

First, in order to confirm the proficiency of the present method, dynamic analysis of FG beams with and without viscoelastic foundation and different boundary conditions are investigated. For this purpose, the numerical results of dynamic analysis CNTRC beams are presented. The beams are composed by Polymethacrylate "PMMA" as matrix and the armchair (10, 10) single walled Carbone nanotubes (SW-CNTs) as reinforcement. The properties of these components are given in Table 2.

Table 3 First three dimensionless natural frequency ϖ $(L/h = 15)$

CNT distribution	Mode	Present study	Lin and Xiang (2014)	Yas and Samadi (2012)
UD-CNT	1	1.4693	1.4348	1.4401
	2	4.2644	4.105	4.1362
	3	7.1756	6.8595	6.9245
FGX-CNT	1	1.6912	1.6409	1.6493
	2	4.6276	4.4333	4.4752
	3	7.5818	7.2258	7.3068
FGʌ-CNT	1	1.2764	1.3975	1.4027
	2	3.9733	3.837	3.8639
	3	6.9501	6.6976	6.7618

Table 4 Comparisons of fundamental frequencies ϖ for CNTRC beams with and without elastic foundation L/h = 15 and $V_{cnt}^{*} = 0.12$

Study	Elastic foundation	CNT distribution			
		UD	O	X	V
Present	$K_w = 0\ ,\ K_s = 0,\ C_d = 0$	0.9925	0.7624	1.1404	0.8581
Wattanasakulpong and Ungbhakorn (2013)		0.9976	0.7628	1.1485	0.8592
Yas and Heshmati (2012),		0.9753	0.7527	1.115	0.9453
Present	$K_w = 0.1\ ,\ K_s = 0.02, C_d = 0$	1.1295	0.9336	1.2614	1.0132
Wattanasakulpong and Ungbhakorn (2013)		1.1339	0.9339	1.2688	1.0142
Yas and Heshmati (2012),		1.1144	0.9258	1.2386	1.0883
Present	$K_w = 0.1, K_s = 0.02\ , C_d = 0.1$	1.1604	0.9709	1.2892	1.0476
	$K_w = 0.1, K_s = 0.02,\ C_d = 0.5$	1.1355	0.9409	1.2668	1.0200
	$K_w = 0.1,\ K_s = 0.02\ ,\ C_d = 1$	1.0537	0.8405	1.1940	0.9282

4.1 Validation

Table 3 presents the first three natural frequencies corresponding to the initial vibration modes of a slender beam (aspect ratio L/h=15) with a carbon nanotube (CNT) volume fraction of Vcnt=0.28. The CNTs are assumed to be distributed according to three distinct patterns: uniform distribution (UD-beam), X-type distribution (X-beam), and Λ -type distribution (Λ-beam). These results are compared with those reported by Lin and Xiang (2014) and Yas and Samadi (2012). It is observed that the present model yields slightly higher frequencies across all distributions and vibration modes, suggesting that the stiffness predicted here is marginally greater than that of the reference studies. This slight overestimation may be attributed to the specific shear correction factor adopted or to the unique kinematic assumptions of the current formulation, which tend to provide a stiffer structural response.

Table 4 shows the dimensionless fundamental frequencies of a functionally graded (FG) beam under carbon nanotube (CNT) distribution patterns, both with and without an elastic foundation. The computed results exhibit strong agreement with benchmark data from Wattanasakulpong and Ungbhakorn (2013) and Yas and Heshmati (2012), as evidenced by the comparative analysis. Notably, our findings consistently fall within the range of values reported in these reference studies, validating the robustness of the present methodology.

4.2 Parametric study

Table 5 presents the fundamental frequencies of CNTRC beams with different CNT distribution patterns (X, O, V, and ʌ) on variable elastic foundations. Frequencies decrease with increasing nonlinearity index for O- and V-type distributions, indicating a softening trend. X- and ʌ-type distributions show increasing frequencies, suggesting that CNTs concentrated toward the surfaces enhance stiffness. Among foundation types, sinusoidal variation consistently yields the highest frequencies due to better stiffness distribution. Parabolic variation generally produces lower frequencies, especially for O- and V-distributed CNTRCs.

The ʌ-distribution exhibits the strongest frequency growth with nonlinearity, showing high sensitivity to foundation effects. X-distributed CNTRCs show the highest overall frequencies across all index values. Figs. 3(a)–(d) illustrate the variation of the wave frequency as a function of the slenderness ratio (L/h). In this analysis, the foundation parameters and the material power-law index (k) were also varied. This investigation was conducted for four distinct CNT distribution patterns: O-beam, X-beam, V-beam, and Λ-beam.The results indicate that the frequency

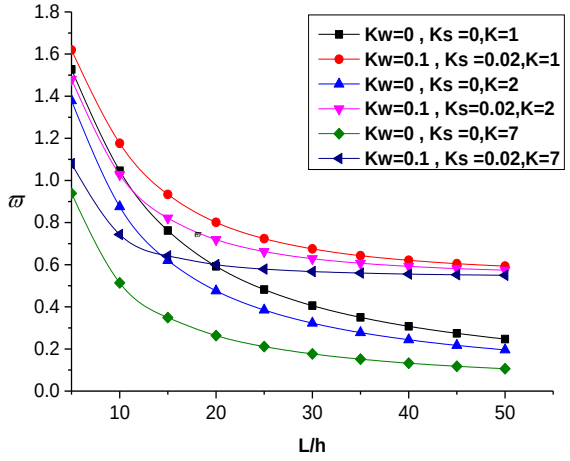

O-beam

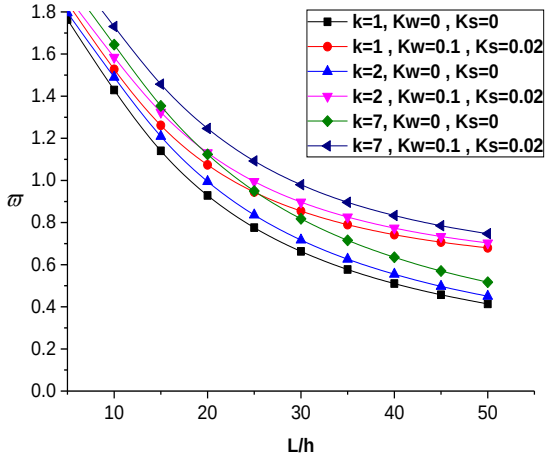

X-beam

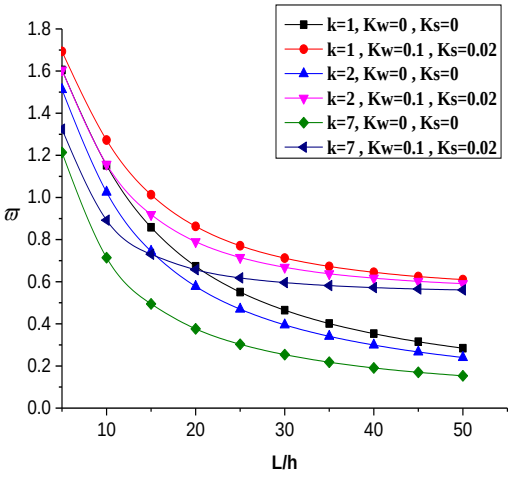

V-beam

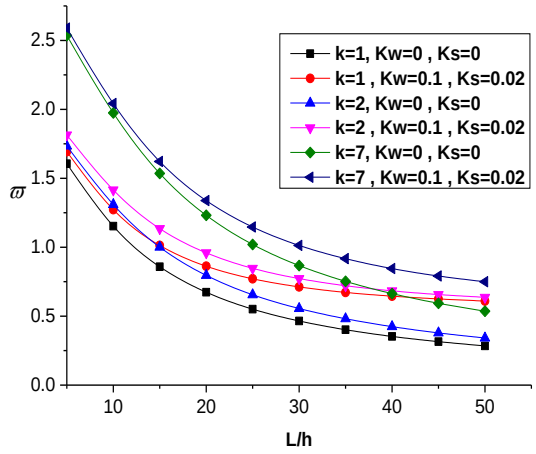

ʌ-beam

Fig. 3 Dimensionless fundamental frequency$\boldsymbol{\varpi}$ of the beam for various thickness ratios $V_{cnt}^{*} = 0.12$

Table 5 Fundamental frequencies ϖ of CNTRC beams on variable elastic foundations with different nonlinearity indices and foundation variation types

Beam	Variation type	Nonlinearity index k					
		1	2	3	4	5	7
O- CNTRC	V-Linear	1.1667	1.0162	0.9142	0.8434	0.7927	0.7279
	V-Sinusodal	1.1752	1.0260	0.9251	0.8551	0.8052	0.7415
	V-Parabolic	1.1513	0.9985	0.8945	0.8219	0.7699	0.7030
X- CNTRC	V-Linear	1.5200	1.5773	1.6122	1.6381	1.6612	1.7242
	V-Sinusodal	1.5265	1.5837	1.6184	1.6442	1.6672	1.7300
	V-Parabolic	1.5081	1.5659	1.6010	1.6271	1.6504	1.7138
V- CNTRC	V-Linear	1.2632	1.1478	1.0590	0.9928	0.9434	0.8794
	V-Sinusodal	1.2710	1.1564	1.0684	1.0027	0.9539	0.8906
	V-Parabolic	1.2489	1.1322	1.0421	0.9747	0.9245	0.8592
ʌ- CNTRC	V-Linear	1.2632	1.4071	1.523	1.6289	1.7371	2.0372
	V-Sinusodal	1.2710	1.4141	1.5294	1.6348	1.7426	2.0418
	V-Parabolic	1.2489	1.3945	1.5114	1.6182	1.7272	2.0289

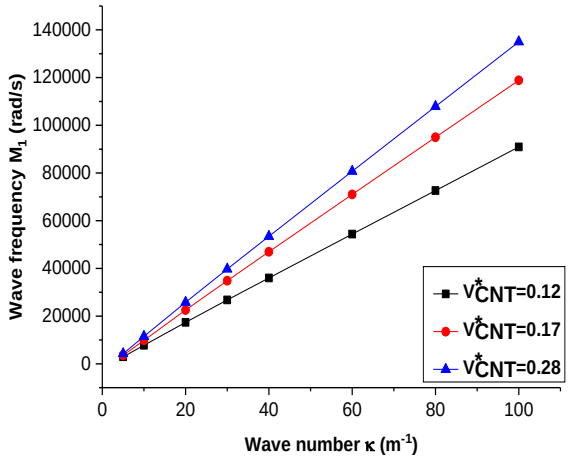

(a) M_0 Mode

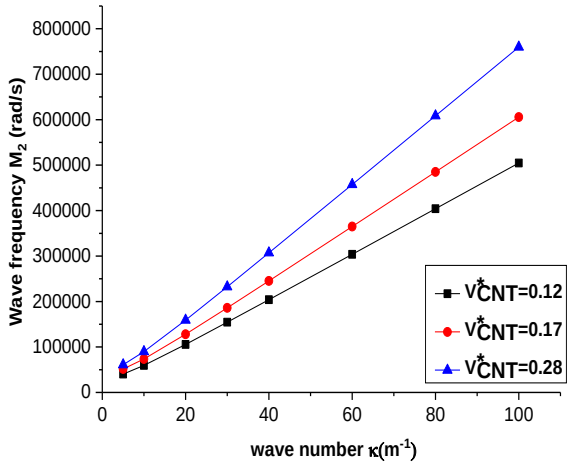

(b) M_1 Mode

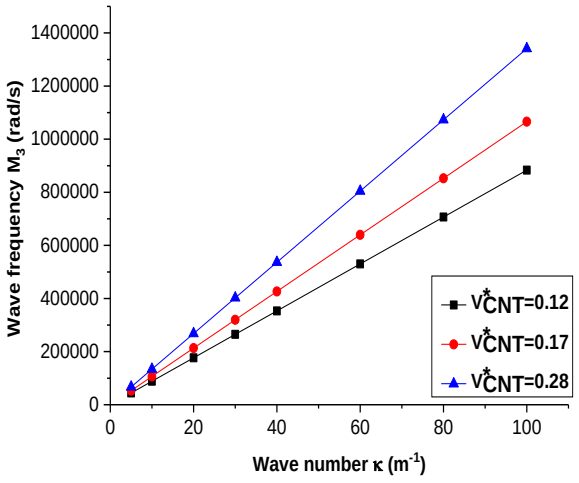

(c) M_2 Mode

Fig. 4 The effects of the CNT volume fraction on the wave frequency and wavenumber dispersion relation in O-Beam, with $K_w = 0.1$, $K_s = 0.01$, $C_d = 0.5$ and L/h=15

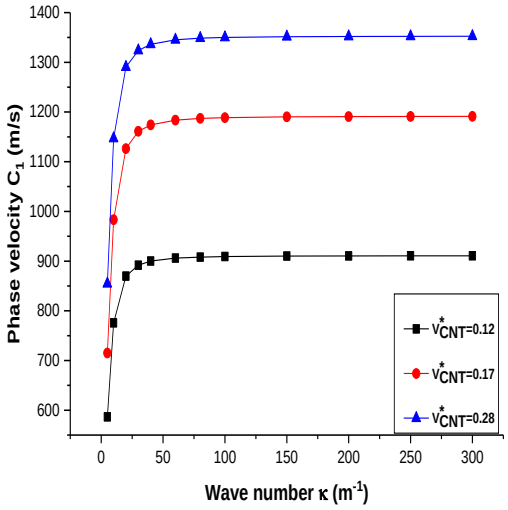

(a) C_0 Mode

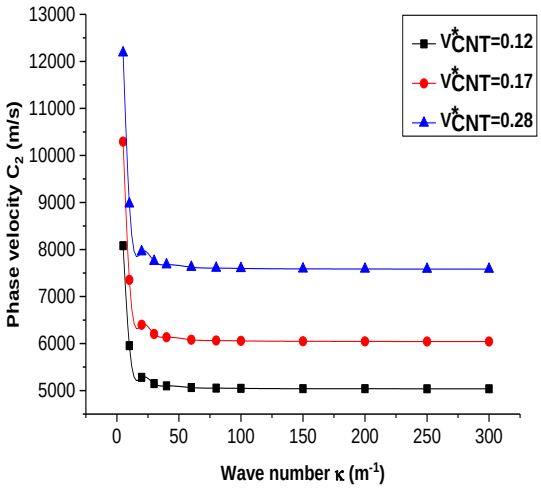

(b) C_2 Mode

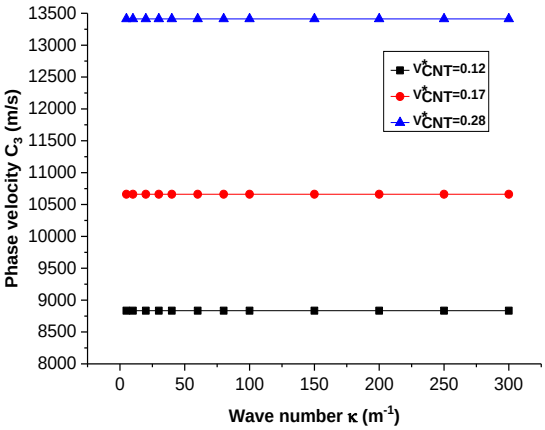

(c) C_3 Mode

Fig. 5 The effects of the CNT volume fraction on the phase velocity and wavenumber dispersion relation in O-Beam, with $K_w = 0.1$, $K_s = 0.01$, $C_d = 0.5$ and $L/h = 15$

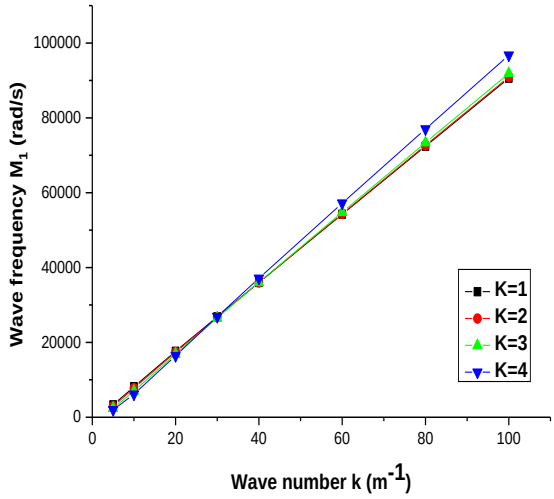

(a) M_0 Mode

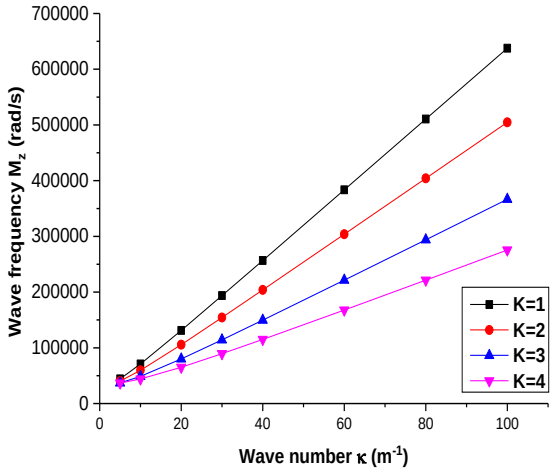

(b) M_2 Mode

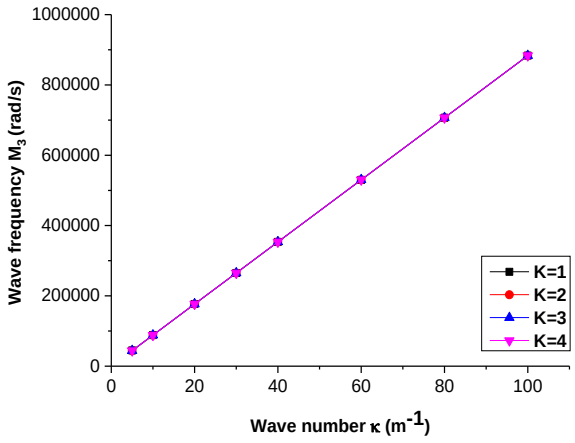

(c) M_3 Mode

Fig. 6 The effects of the CNT's nonlinearity index on the wave frequency and wavenumber dispersion relation in O-Beam, with $K_w = 0.1$, $K_s = 0.01$, $C_d = 0.5$ and $L/h = 15$

decreases as the slenderness ratio (L/h) increases. This reduction is more pronounced for thick plates, whereas for higher L/h values, the rate of frequency decline diminishes. Notably, the presence of an elastic foundation increases the plate's vibrational frequency, indicating enhanced structural.

Furthermore, the influence of the material index (k) exhibits distribution-dependent behavior: an increase in k leads to a reduction in the fundamental frequency for O- and V-beam distributions, whereas for X- and Λ-beam distributions, the fundamental frequency increases with higher k. Fig. 4 illustrates the frequency dispersion characteristics of the first three vibrational modes versus wavenumber for an O-pattern carbon nanotube-reinforced beam (CNT volume fraction Vcnt) with a material gradient index k = 2, supported on a Winkler-Pasternak foundation (slenderness ratio L/h = 15). The results demonstrate: (i) a quasi-linear relationship between frequency and wavenumber across all vibrational modes, (ii) a systematic increase in natural frequencies (depending on mode) with increasing CNT volume fraction Vcnt, attributable to enhanced beam stiffness through improved composite elastic modulus, effective CNT–matrix load transfer, and \constrained matrix deformation. The observed quasi-linear trend at low κ values corresponds to shear-dominated wave propagation, whereas deviations at higher κ reflect the dispersive nature of bending waves, which become increasingly significant at larger wavenumbers.

Fig. 5 presents the phase velocity evolution of the first three vibration modes as a function of wavenumber for an O-pattern carbon nanotube-reinforced beam with varying CNT volume fractions (Vcnt). The beam features a material gradient index of k = 2, is supported on a Winkler-Pasternak foundation, and has a slenderness ratio of L/h = 15. Key observations include: (i) a quasi-linear relationship between phase velocity and wavenumber for the fundamental mode, and (ii) a systematic increase in phase velocity with higher Vcnt values, which is attributed to enhanced beam stiffness resulting from CNT reinforcement. The linear trend of C = ω/κ at small κ values indicates shear-controlled propagation with nearly constant phase velocity, while the gradual deviations observed at higher κ highlight the onset of bending-induced dispersion, thereby reconciling the apparent discrepancy between Figs. 4 and 5.

Fig. 6 illustrates the frequency dispersion characteristics of an O-pattern CNT-reinforced beam (k=2) resting on a Winkler–Pasternak elastic foundation, with particular emphasis on the influence of the material gradient index (k). The results indicate a consistent quasi-linear relationship between the natural frequency and the wavenumber across all vibrational modes, confirming the fundamental wave propagation trends observed in Fig. 4. For the fundamental mode (Mode I), a slight frequency increase of approximately 3–5% is obtained with higher material index values. This enhancement is mainly attributed to the graded variation of material properties through the beam thickness, which modifies the elastic energy distribution and improves the stiffness characteristics as a result of functional gradation.

Fig. 7 illustrates the influence of the CNT nonlinearity

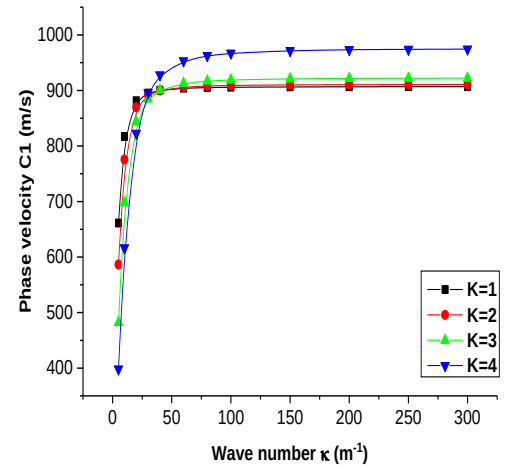

(a) C_0 Mode

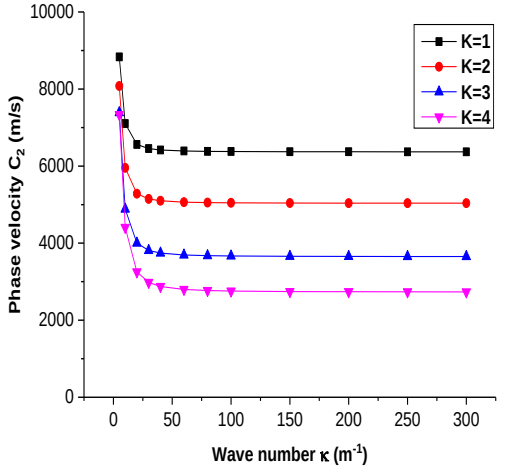

(b) C_2 Mode

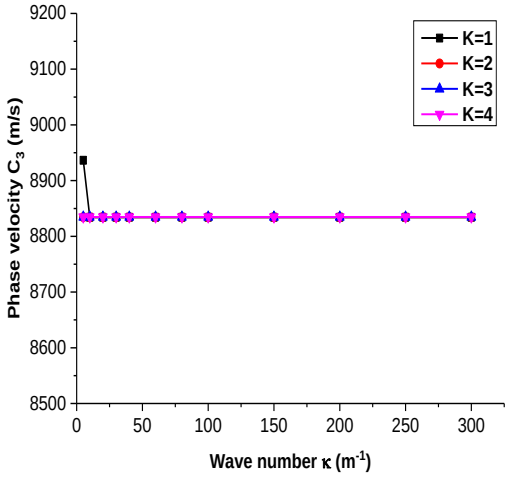

(c) C_3 Mode

Fig. 7 The effects of the CNT's nonlinearity index on the phase velocity and wavenumber dispersion relation in O-Beam, with $K_w = 0.1$, $K_s = 0.01$, $C_d = 0.5$ and $L/h = 15$

index (*K=1–4*) on the phase velocity–wavenumber dispersion of an O-pattern CNTRC beam resting on a viscoelastic foundation. It is observed that for the first mode (C_1), the phase velocity increases rapidly with the wavenumber and tends toward a constant asymptotic value. A higher nonlinearity index K leads to greater velocities, indicating an effective enhancement of the beam stiffness. For the second mode (C_2), the phase velocity decreases sharply at low wavenumbers and subsequently stabilizes. In this case, increasing *K* reduces the velocity levels, highlighting the stronger dispersive effects induced by CNT nonlinearity. For the third mode (C_3), the phase velocity remains nearly invariant with respect to both wavenumber and *K*. Overall, these results suggest that tailoring CNT nonlinearity can be an efficient strategy to tune the wave propagation behavior of CNTRC beams, especially in vibration control and dynamic stability applications.

5. Conclusions

This investigation has provided a detailed analytical study on the wave propagation behavior of carbon nanotube-reinforced composite (CNTRC) beams resting on spatially varying viscoelastic foundations. By employing the integral-first shear deformation theory (IFSDT) within Hamilton's principle, dispersion relations were derived to assess the effects of CNT distribution configurations, volume fraction, and foundation characteristics on the dynamic response of functionally graded beams. Unlike the classical FSDT, which relies on a constant shear correction factor, the IFSDT derives the shear parameter k_1 directly from the harmonic solution, making the formulation wave–number dependent and better suited to capture scale-sensitive shear effects in wave propagation problems. The results, validated through comparison with benchmark studies, exhibit excellent agreement, thereby confirming the reliability and accuracy of the proposed model. It was observed that X-type and Λ-type CNT distributions significantly enhance the structural stiffness and natural frequencies, particularly with increasing nonlinearity indices, while O- and V-type distributions display softening behavior. Additionally, sinusoidal variations in the foundation stiffness consistently yielded higher frequencies compared to linear and parabolic profiles. The inclusion of CNT volume fraction and gradient index (**k**) further amplified both frequency and phase velocity, attributed to enhanced modulus, effective load transfer, and reduced matrix deformation. The analysis also confirmed a quasi-linear relationship between frequency/phase velocity and wavenumber. It should be noted that the present study, based on FSDT, is most suitable for slender to moderately thick beams, while very thick beams would require higher-order shear deformation theories. Moreover, environmental effects such as temperature and humidity were not considered, although they may significantly influence the mechanical response of CNT-reinforced composites. Future research should extend the analysis to alternative boundary conditions to enhance the generality and applicability of the findings. Incorporating environmental influences and higher-order models would further improve accuracy.

Finally, experimental validation is strongly recommended to confirm the practical reliability of the proposed theoretical framework.

References

Asgari, G.R., Arabali, A., Babaei, M. and Asemi, K. (2022), "Dynamic instability of sandwich beams made of isotropic core and functionally graded graphene platelets-reinforced composite face sheets", *Int. J. Struct. Stabil. Dyn.*, **22**(8), 2250092. https://doi.org/10.1142/s0219455422500924

Djilali Djebbour, K., Mokhtar, N., Hassen, A.A., Alghanmi, R.A., Hadji, L. and Riadh, B. (2024), "An enhanced quasi-3D HSDT for free vibration analysis of porous FG-CNT beams on a new concept of orthotropic VE-foundations", *Mech. Adv. Mater. Struct.*, 1-17. https://doi.org/10.1080/15376494.2024.2356728

Frahlia, H., Bennai, R., Nebab, M., Ait Atmane, H. and Tounsi, A. (2023), "Assessing effects of parameters of viscoelastic foundation on the dynamic response of functionally graded plates using a novel HSDT theory", *Mech. Adv. Mater. Struct.*, **30**(13), 2765-2779. https://doi.org/10.1080/15376494.2022.2062632

Ghayoumizadeh, H., Shahabian, F. and Hosseini, S.M. (2013), "Elastic wave propagation in a functionally graded nano-composite reinforced by carbon nanotubes employing meshless local integral equations (LIEs)", *Eng. Anal. Bound. Elem.*, **37**(11), 1524-1531. https://doi.org/10.1016/j.enganabound.2013.08.011

Ghorbanpour Arani, A., Jamali, M., Mosayyebi, M. and Kolahchi, R. (2016), "Wave propagation in FG-CNT-reinforced piezoelectric composite micro plates using viscoelastic quasi-3D sinusoidal shear deformation theory", *Compos. Part B Eng.*, **95**, 209-224. https://doi.org/10.1016/j.compositesb.2016.03.077

Han, Y. and Elliott, J. (2007), "Molecular dynamics simulations of the elastic properties of polymer/carbon nanotube composites", *Comput. Mater. Sci.*, **39**(2), 315-323. https://doi.org/10.1016/j.commatsci.2006.06.011

Hu, N., Fukunaga, H., Lu, C., Kameyama, M. and Yan, B. (2005), "Prediction of elastic properties of carbon nanotube reinforced composites", *Proceedings of the Royal Society A: Mathematical, Physical and Engineering Sciences*, **461**(2058), 1685-1710. https://doi.org/10.1098/rspa.2004.1422

Ke, L.L., Yang, J. and Kitipornchai, S. (2010), "Nonlinear free vibration of functionally graded carbon nanotube-reinforced composite beams", *Compos. Struct.*, **92**(3), 676-683. https://doi.org/10.1016/j.compstruct.2009.09.024

Kehli, A., Nebab, M., Bennai, R., Ait Atmane, H. and Dahmane, M. (2024), "Dynamic characteristics analysis of functionally graded cracked beams resting on viscoelastic medium using a new quasi-3D HSDT", *Mech. Adv. Mater. Struct.*, 1-14. https://doi.org/10.1080/15376494.2024.2326983

Kenza Djilali, D., Mokhtar, N., Mehmet, A., Hassen, A.A., Fabrice, B., Riadh, B. and Burak, İ. (2025), "Stability and vibration analysis of shear deformable FG-CNTRC beams resting on elastic foundations", *Adv. Nano Res.*, **18**(3), 205-221. https://doi.org/10.12989/anr.2025.18.3.205

Kolahchi, R., Zarei, M.S., Hajmohammad, M.H. and Nouri, A. (2017), "Wave propagation of embedded viscoelastic FG-CNT-reinforced sandwich plates integrated with sensor and actuator based on refined zigzag theory", *Int. J. Mech. Sci.*, **130**, 534-545. https://doi.org/10.1016/j.ijmecsci.2017.06.039

Lau, A.K.T. and Hui, D. (2002), "The revolutionary creation of new advanced materials—carbon nanotube composites", *Compos. Part B Eng.*, **33**(4), 263-277. https://doi.org/10.1016/S1359-8368(02)00012-4

Lin, F. and Xiang, Y. (2014), "Vibration of carbon nanotube reinforced composite beams based on the first and third order beam theories", *Appl. Math. Modell.*, **38**(15), 3741-3754. https://doi.org/10.1016/j.apm.2014.02.008

Mehar, K. and Panda, S.K. (2016), "Thermoelastic analysis of FG-CNT reinforced shear deformable composite plate under various loadings", *Int. J. Comput. Meth.*, **14**(2), 1750019. https://doi.org/10.1142/S0219876217500190

Mellal, F., Bennai, R., Nebab, M., Atmane, H.A., Bourada, F., Hussain, M. and Tounsi, A. (2024), "Investigation on the effect of porosity on wave propagation in FGM plates resting on elastic foundations via a quasi-3D HSDT", *Waves Random Complex Med.*, **34**(5), 3727-3753. https://doi.org/10.1080/17455030.2021.1983235

Nebab, M., Ait Atmane, H., Bennai, R. and Tahar, B. (2019a), "Effect of nonlinear elastic foundations on dynamic behavior of FG plates using four-unknown plate theory", *Earthq. Struct.*, **17**(5), 447-462. https://doi.org10.12989/eas.2019.17.5.447

Nebab, M., Ait Atmane, H., Bennai, R. and Tounsi, A. (2019b), "Effect of variable elastic foundations on static behavior of functionally graded plates using sinusoidal shear deformation", *Arab. J. Geosci.*, **12**(24), 809. https://doi.org10.1007/s12517-019-4871-5

Nebab, M., Dahmane, M., Belqassim, A., Atmane, H.A., Bernard, F., Benadouda, M., Bennai, R. and Hadji, L. (2024a), "Fundamental frequencies of cracked FGM beams with influence of porosity and Winkler/Pasternak/Kerr foundation support using a new quasi-3D HSDT", *Mech. Adv. Mater. Struct.*, **31**(28), 10639-10651. https://doi.org/10.1080/15376494.2023.2294371

Nebab, M., Hassen, A.A., Riadh, B. and Mouloud, D. (2024b), "Warping and porosity effects on the mechanical response of FG-Beams on non-homogeneous foundations via a Quasi-3D HSDT", *Struct. Eng. Mech.*, **90**(1), 83-94. https://doi.org/10.12989/sem.2024.90.1.083

Nejati, M., Eslampanah, A. and Najafizadeh, M. (2016), "Buckling and vibration analysis of functionally graded carbon nanotube-reinforced beam under axial load", *Int. J. Appl. Mech.*, **8**(1), 1650008. https://doi.org/10.1142/s1758825116500083

Nguyen, X.T., Hoang-Le, M., Khatir, S., Tran, M.T. and Cuong-Le, T. "A new modified couple stress finite element model for buckling analysis of laminated CNTs-reinforced composite microplate", *Int. J. Struct. Stabil. Dyn.*, 2650117. https://doi.org/10.1142/s0219455426501178

Pouresmaeeli, S., Ghavanloo, E. and Fazelzadeh, S.A. (2013), "Vibration analysis of viscoelastic orthotropic nanoplates resting on viscoelastic medium", *Compos. Struct.*, **96**, 405-410. https://doi.org/10.1016/j.compstruct.2012.08.051

Setoodeh, A., Shojaee, M. and Malekzadeh, P. (2019), "Vibrational behavior of doubly curved smart sandwich shells with FG-CNTRC face sheets and FG porous core", *Compos. Part B Eng.*, **165**, 798-822. https://doi.org/10.1016/j.compositesb.2019.01.022

Syduzzaman, M., Islam Saad, M.S., Piam, M.F., Talukdar, T.A., Shobdo, T.T. and Pritha, N.M. (2025), "Carbon nanotubes: Structure, properties and applications in the aerospace industry", *Results Mater.*,. **25**, 100654. https://doi.org/10.1016/j.rinma.2024.100654

Tao, Y., Teng, Q. and Long, L. "Numerical solution for dynamic analysis of multi-scale hybrid stepped annular plates reinforced with cf and agglomerated GPLs", *Int. J. Struct. Stabil. Dyn.*, Online Ready. https://doi.org/10.1142/s0219455426502391

Thostenson, E.T., Ren, Z. and Chou, T.W. (2001), "Advances in the science and technology of carbon nanotubes and their composites: A review", *Compos. Sci. Technol.*, **61**(13), 1899-1912. https://doi.org/10.1016/S0266-3538(01)00094-X

Wattanasakulpong, N. and Ungbhakorn, V. (2013), "Analytical solutions for bending, buckling and vibration responses of carbon nanotube-reinforced composite beams resting on elastic

foundation", *Comput. Mater. Sci.*, **71**, 201-208. https://doi.org/10.1016/j.commatsci.2013.01.028

Wu, H., Kitipornchai, S. and Yang, J. (2015), "Free vibration and buckling analysis of sandwich beams with functionally graded carbon nanotube-reinforced composite face sheets", *Int. J. Struct. Stabil. Dyn.*, **15**(7), 1540011. https://doi.org/10.1142/S0219455415400118

Xie, X.L., Mai, Y.W. and Zhou, X.P. (2005), "Dispersion and alignment of carbon nanotubes in polymer matrix: A review", *Mater. Sci. Eng. R.*, **49**(4), 89-112. https://doi.org/10.1016/j.mser.2005.04.002

Yamamoto, N., Guzman de Villoria, R. and Wardle, B.L. (2012), "Electrical and thermal property enhancement of fiber-reinforced polymer laminate composites through controlled implementation of multi-walled carbon nanotubes", *Compos. Sci. Technol.*, **72**(16), 2009-2015. https://doi.org/10.1016/j.compscitech.2012.09.006

Yas, M.H. and Heshmati, M. (2012), "Dynamic analysis of functionally graded nanocomposite beams reinforced by randomly oriented carbon nanotube under the action of moving load", *Appl. Math. Modell.*, **36**(4), 1371-1394. https://doi.org/10.1016/j.apm.2011.08.037

Yas, M.H. and Samadi, N. (2012), "Free vibrations and buckling analysis of carbon nanotube-reinforced composite Timoshenko beams on elastic foundation", *Int. J. Press. Vessels Piping*, **98**, 119-128. https://doi.org/10.1016/j.ijpvp.2012.07.012

Zouatnia, N., Hadji, L., Atmane, H.A., Nebab, M., Madan, R., Bennai, R. and Dahmane, M. (2024), "Analysis of free vibration in bi-directional power law-based FG beams employing RSD theory", *Coupled Syst. Mech.*, **13**(4), 359. https://doi.org/10.12989/csm.2024.13.4.359

CC